

# Synthesis and Characterization of Poly(methyl acrylate) Grafted from Poly(thiophene) to Form Solid-State Fluorescent Materials

Philip J. Costanzo<sup>\*,†</sup> and Kristoffer K. Stokes<sup>\*,‡</sup>

Center of Macromolecule Engineering, Department of Chemistry, Carnegie Mellon University, 4400 Fifth Avenue, Pittsburgh, Pennsylvania 15213

Received September 17, 2001; Revised Manuscript Received April 29, 2002

**ABSTRACT:** This paper describes the synthesis and characterization of graft copolymers having a poly-(thiophene) (PT) backbone with poly(methyl acrylate) (pMA) sidearms. Thiophene monomer containing a protected alcohol group was prepared and polymerized via the McCullough method to yield regioregular PT. The backbone was then functionalized to contain an atom-transfer radical polymerization (ATRP) initiator at approximately 90% of the repeat units as determined through <sup>1</sup>H NMR analysis, yielding 2,5-poly(3-[1-ethyl-2-(2-bromopropionate)]thiophene). From these initiator sites, MA was polymerized to yield well-defined polymer brushes. The addition of the sidearms to the thiophene backbone resulted in twisting of the backbone as a result of steric effects, which caused a decrease in conjugation length of the PT. In the solid state, the sidearms trap the PT in a "solution-like" conformation. In addition, these arms serve to separate PT chains and disrupt the ordered array usually seen in regioregular PT. With a lower conjugation length and isolated PT chains, the material achieved a photoluminescent yield of up to 40% in the solid state.

## Introduction

Since the discovery of conductive polymers in 1977,<sup>1</sup> a considerable amount of research has been focused on these materials and their applications, including wholly organic field-effect transistors,<sup>2</sup> rechargeable batteries,<sup>3</sup> light-emitting diodes (LEDs),<sup>4</sup> integrated circuits,<sup>5</sup> and chemosensors.<sup>6</sup> For a polymer to conduct, it must have a conjugated  $\pi$  system along the backbone, but this adds rigidity to the polymer, which makes processing extremely difficult.

One way to improve the processability of a polymer such as poly(thiophene) (PT) is to incorporate processable segments such as poly(styrene),<sup>7,8</sup> poly(methacrylate)s,<sup>9,10</sup> poly(acrylate),<sup>11</sup> and poly(dimethylsiloxane).<sup>12</sup> These segments will directly affect the properties of the PT. Removal of the segments can leave insoluble PT with a high conductivity. However, if the segments remain, the photoluminescent properties of the PT can be enhanced. Typical solid-state fluorescence in PT is low, with a quantum yield of approximately 1–3%.<sup>13</sup> However, dispersion within the polymer matrix reduces  $\pi$ -stacking interactions, which improves the photoluminescent properties.<sup>14,15</sup> This principle of separating PT chains and other conductive polymers by bulky side chains and polymerization defects to increase photoluminescence has also been noted previously.<sup>16–22</sup> Previous attempts also utilized block copolymers and blends to inhibit  $\pi$ -stacking, but aggregated regions were still present as a result of microphase separation.<sup>23–27</sup>

There are three techniques in synthesizing graft polymers with a comblike structure: grafting through a macromonomer, grafting from a functional backbone,

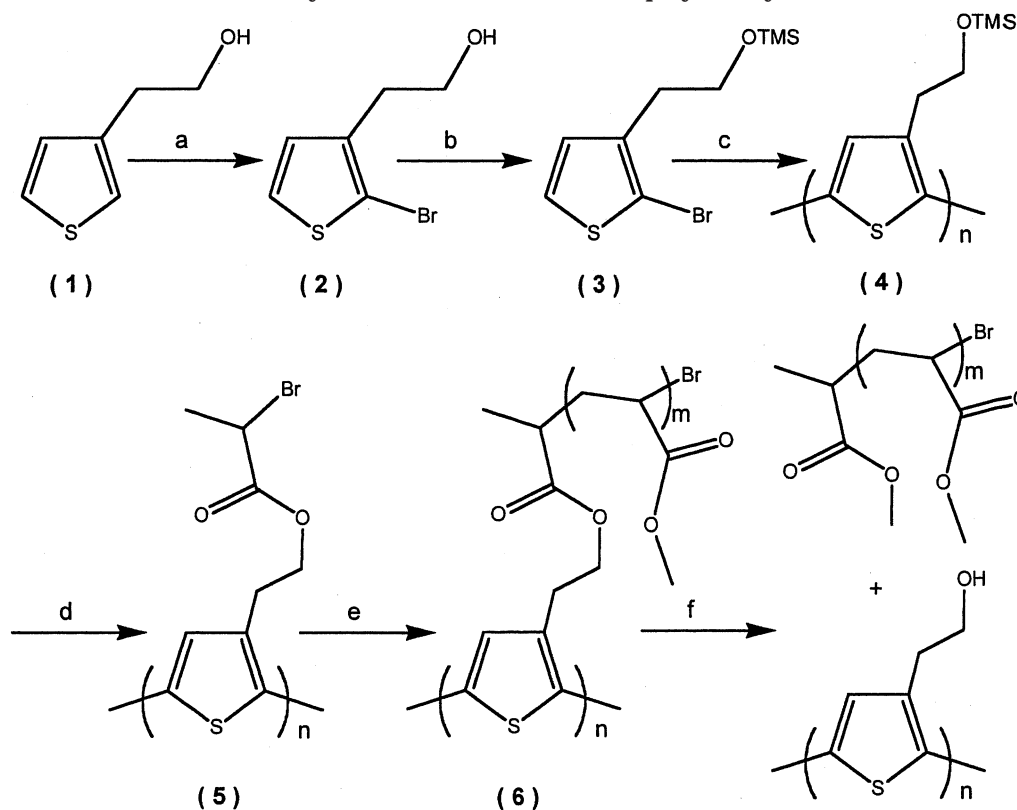
and grafting onto a functional backbone. To our knowledge, two techniques have been attempted in synthesizing comblike molecules containing PT: grafting through a macromonomer<sup>10,12,28</sup> and grafting from the backbone.<sup>7,9,11</sup> In most of these attempts, PT was incorporated within the graft copolymer by utilizing a flexible vinyl polymer and then grafting PT arms from randomly dispersed intervals throughout the backbone. In each of these attempts, the backbone was prepared by a free-radical polymerization, and thiophene was then oxidatively polymerized with FeCl<sub>3</sub> from the backbone. Both of these steps provide limited control over the molecular weight distribution (MWD), do not control the regioregularity of PT, and lead to limited success with conductivity and fluorescent properties. Frechet's work<sup>28</sup> utilized PT as the backbone of the graft copolymer and achieved superb conductivity while maintaining solubility. Here, the dendrimer sidearm was prepared before the PT backbone in a grafting-through technique.

In using the grafting-from approach, one has greater control of the backbone variables including functionality, composition, size, and MWD. As previously mentioned, PT prepared via oxidative polymerization results in a nonregioregular PT that has a large MWD. It has been shown that regioregular PT exhibits electroluminescent properties superior to those of nonregioregular PT.<sup>29</sup> Regioregular PT can also create a featherlike structure in which the substituents, if large enough, could isolate the PT chains from each other. Use of the McCullough method<sup>30</sup> can yield PT with high regioregularity (head-to-tail coupling > 95%)<sup>30–32</sup> with a MWD much lower than that of the oxidatively prepared PT. However, formation of the comblike structure typically results in a loss of synthetic control over the MWD. If a living/controlled process is used for the sidearms, then this difficulty can be reduced or even eliminated. Controlled radical polymerizations, particularly atom-transfer radical polymerization (ATRP), yield materials of controlled molecular weight<sup>33,34</sup> with low polydispersities<sup>35</sup> and are applicable to many types of monomers,

\* Address correspondence to Richard D. McCullough at Carnegie Mellon University. Inquires will then be forwarded to the authors.

<sup>†</sup> Current address: Department of Chemistry, University of California at Davis, One Shields Ave., Davis, CA 95616-5295.

<sup>‡</sup> Current address: Department of Chemistry, Massachusetts Institute of Technology, 77 Massachusetts Avenue, Cambridge, MA 02139.

Scheme 1. Synthetic Scheme of Graft Copolymer Synthesis<sup>a</sup>

<sup>a</sup> Conditions: (a) NBS, THF; (b) NEt<sub>3</sub>, Me<sub>3</sub>SiCl, THF; (c) 1, LDA, THF; 2, ZnCl<sub>2</sub>; 3, Ni(dppp)Cl<sub>2</sub>; (d) THF, NEt<sub>3</sub>, TBAF, 2-bromopropionyl bromide; (e) ATRP conditions; (f) H<sub>2</sub>SO<sub>4</sub>, THF, MeOH.

such as (meth)acrylates, styrene, and acrylonitrile. There have been reports of brush polymer synthesis by grafting from the backbone to form side chains of various compositions using ATRP conditions.<sup>36,37</sup>

Our idea was to incorporate a high density of solubilizing segments by addition to every repeat unit rather than only a few units per chain. We report a graft copolymer utilizing PT with poly(methyl acrylate) (pMA) grafts synthesized via Scheme 1. The pMA sidearms separate the PT backbones and inhibit any  $\pi$ -stacking interactions, which improves the photoluminescent properties.

## Results and Discussion

Two different synthetic techniques were explored in the preparation of the graft copolymers. The most important aspect of the synthesis was the method of incorporation of the ATRP initiator. Maximum functionality of the macroinitiator could be ensured by polymerization of ATRP-functional thiophene. However, homopolymerizations of **7** and **8** (Figure 1) yielded no polymer. The two most plausible explanations for the failed polymerization of **7** are the following: (1) the formation of enol rather than 5-lithiothiophene and (2) the involvement of the labile Br group in a metal-halogen exchange instead of lithiation at the 5 position. Compound **8** would eliminate enol formation. Therefore, we believe that Br exchange is more favorable than lithiation at the 5 position on the thiophene, which terminates the polymerization at the monomer stage.

Therefore, Scheme 1 was followed, in which monomer **3** was polymerized into regioregular PT via a modified McCullough method. The original McCullough method produces a lithiated thiophene that then undergoes

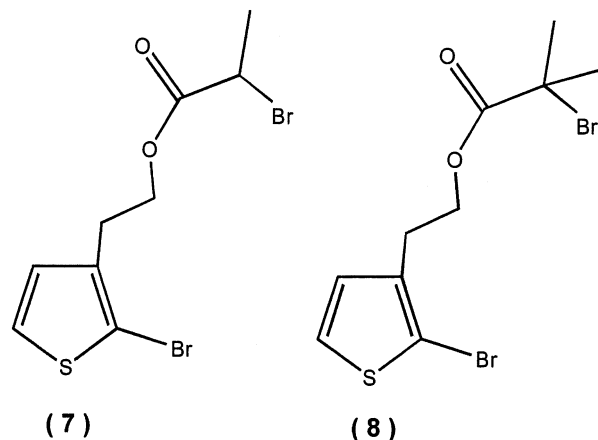


**Figure 1.** Structures of ATRP-functional thiophene monomers.

transmetalation with magnesium bromide etherate. Cross coupling is then completed with a nickel catalyst.<sup>30</sup> In the modified method used here, zinc chloride was used for the transmetalation for enhanced functional group tolerance. Polymer **4** was then deprotected and functionalized into an ATRP macroinitiator. A key aspect in macroinitiator functionalization is that removal of the protecting group and addition of the ATRP initiator must take place in the same step, because the deprotected hydroxy polymer is insoluble in any solvent.<sup>38,39</sup> To avoid precipitation of the backbone, 2-bromopropionyl bromide was added in excess before the tetrabutylammonium fluoride cleavage agent, which resulted in the highest degree of functionalization (see Table 1).

<sup>1</sup>H NMR spectroscopy of **4** could not be completed because of solubility problems, and therefore, model

**Table 1. Functionalization Data of the Prepared ATRP-Functional PT Macroinitiator**

sample	conversion (%)	functionality (%)	$M_n$ (g/mol) of pMA sidearms			
			GPC	NMR <sup>a</sup>	Theo{Actual} <sup>b</sup>	Theo{100%} <sup>c</sup>
1 <sup>d</sup>	36	53	13 000	10 500	9710	5500
4 <sup>e</sup>	19	86	5300	3900	3500	2900

<sup>a</sup> As determined from GPC and <sup>1</sup>H NMR analyses (described in the text.). <sup>b</sup> Theoretical  $M_n$  based on determined functionality of PT backbone. <sup>c</sup> Theoretical  $M_n$  based on 100% functionality of **5**. <sup>d</sup> Functionalization conditions: addition of TBAF, NEt<sub>3</sub>, and 2-bromopropionyl bromide, in that order. <sup>e</sup> Functionalization conditions: addition of 2-bromopropionyl bromide, NEt<sub>3</sub>, and TBAF, in that order.

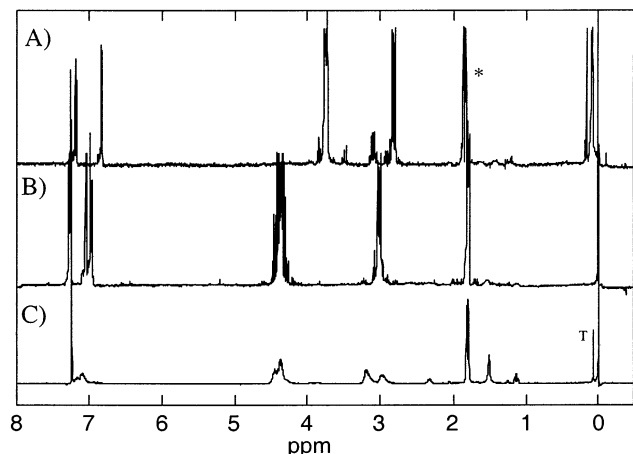


**Figure 2.** <sup>1</sup>H NMR spectra: (A) unprotected and TMS protected thiophene monomer; (B) ATRP functional thiophene monomer; (C) compound **5**, which shows ~86% functionalization of **5**. The asterisk denotes solvent and NEt<sub>3</sub> impurities.

compounds were prepared to show incorporation of the ATRP initiator into the PT. <sup>1</sup>H NMR analyses of the compounds **3**, **5**, and **7** were completed to determine the extent of macroinitiator functionality. As seen in Figure 2, peaks resulting from the α-bromo ester have been incorporated into **5**, showing some degree of functionalization.

However, complete functionalization was not achieved because of the difficulty in postpolymerization functionalization. Incomplete functionalization can be seen by comparing the unprotected thiophene monomer **2** and the trimethylsiloxy (OTMS)-protected monomer **3** to **5**. Peak T indicates the presence of tetramethylsilane (TMS) added as an internal standard and the OTMS protecting group (see Figure 2). According to the <sup>1</sup>H NMR analysis, the backbone attained 86% functionality. Determination of backbone functionality will be discussed in further detail later in this paper. From the known degree of functionalization, the amount of initiator present was determined, and appropriate ATRP conditions to polymerize MA on PT were developed.

During the ATRP step, three techniques were used to avoid irreversible termination reactions, such as brush–brush coupling: the addition of Cu<sup>II</sup>, the use of a high monomer concentration, and the addition of solvent. Addition of Cu<sup>II</sup> helps to avoid termination reactions by the persistent radical effect.<sup>40</sup> In the initial polymerizations, Cu<sup>II</sup> was apparently not being efficiently transferred into the reaction flask. Therefore, Cu<sup>II</sup> was loaded into the reaction flask to ensure the presence of deactivator, which resulted in a lowering of the polydispersity of the sidearms, as seen in Table 2 from samples 1 and 4. A high monomer concentration allows the reaction to be stopped at low conversion, which reduces possible side reactions, such as brush–brush coupling, and is typical for the formation of brush molecules using ATRP.<sup>36,37</sup> Finally, the addition of

anisole helped to reduce the incompatibility between the thiophene backbone and the methyl acrylate monomer. However, an appropriate solvent was not found to solubilize high-molecular-weight PT and be effective for ATRP. In the preparation of sample **3**, a large amount of PT precipitated out of solution at room temperature. However, upon heating, the polymerization was initiated, and the solution became homogeneous. As sidearms began to grow, the solubility of the PT was enhanced, which increased the amount of initiator present in solution. An increase in initiator resulted in an increase in the number of radicals formed, which led to irreversible termination reactions and a larger polydispersity index (PDI). Table 2 lists the ATRP conditions and molecular weight data for the graft copolymers synthesized.

To confirm that the pMA was covalently bonded to the PT, the <sup>1</sup>H NMR spectra of **5** and **6** were compared. Peak C in Figure 3 relates to the methoxy protons from poly(methyl acrylate). The shift of peak B from 4.2 ppm to between 1 and 3 ppm, which is caused by replacement of a Br atom with a repeat unit, indicates that the polymer was indeed grafted to the PT and not free in solution. Each chain is still terminated with a Br, resulting in peak D, but the intensity of this peak is very small because of the relative number of pMA backbone protons to pMA chain-end protons.

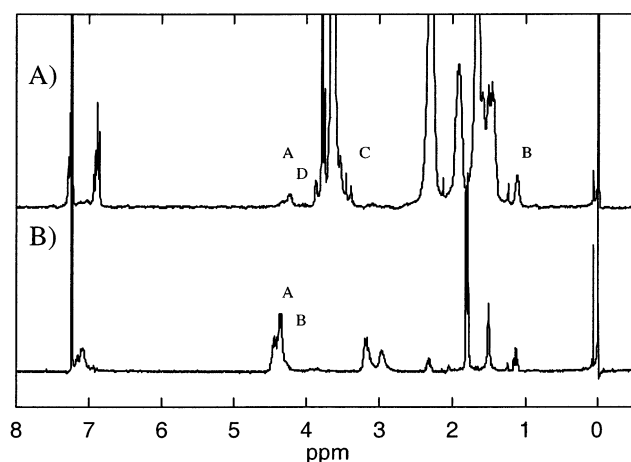
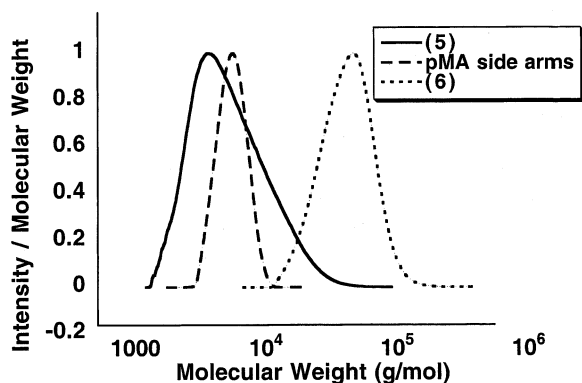
Figure 4 presents the results of GPC analyses of **5** and **6**, which indicate a clear shift to a higher-molecular-weight polymer and thus the absence of irreversible termination reactions. The pMA grafts were also analyzed by GPC after transesterification of the ester linkage between the backbone and ATRP initiator (Scheme 1). Analysis of the cleaved grafts shows that growth occurred in a controlled manner, yielding polymers of low polydispersity with predetermined molecular weights. As seen in Table 2, there are large inconsistencies in the molecular weight and PDI of **5**. Molecular weight data were collected using both chloroform (Table 2, PT macroinitiator **5**, first column) and THF (Table 2, PT macroinitiator **5**, second column) eluents with a UV/vis and a refractive index detector, respectively. These variations in the molecular weights and PDIs are most likely caused by the poor solubilization of PT in THF, which most likely leads to aggregation of PT. Analysis of **5** using chloroform as the eluent resulted in more reliable molecular weight and polydispersity measurements. However, for **6**, the pMA side chains displayed good solubility in THF and helped to solvate the PT. This separated the PT and created an artificial decrease of the PDI from **5** to **6**. Another possible explanation for the decrease in PDI is the poor solubility of high-molecular-weight PT in anisole. In the polymerization of sample **3**, a large amount of PT backbone precipitated out of solution; this would result in fractionation of the polymer sample and a lower PDI. These issues of PT solubility can most likely account for the results shown in Table 2. The graft copolymers

**Table 2.** Reaction Conditions for ATRP of MA from PT Macroinitiator

sample <sup>a</sup>	time (min)	conversion (%)	$M_n$ (g/mol) ( $M_w/M_n$ ) <sup>b</sup>			
			PT macroinitiator <b>5</b> <sup>c</sup>	arms <sup>d</sup>	graft copolymer <b>6</b> <sup>d</sup>	
1	100	16	7200 (1.7)	8800 (5.1)	N/A	64 000 (1.4)
	315	36	7200 (1.7)	8800 (5.1)	13 000 (3.1)	68 000 (4.8)
2	90	10	5200 (2.1)	8100 (2.9)	N/A	51 500 (2.7)
	180	32	5200 (2.1)	8100 (2.9)	N/A	67 700 (2.3)
3 <sup>e</sup>	315	12	13 000 (1.9)	13 000 (2.6)	N/A	44 600 (2.9)
4 <sup>e</sup>	145	19	5200 (2.1)	8100 (2.9)	5300 (1.07)	44 000 (1.21)

<sup>a</sup> [M]/[I]/[Cu<sup>I</sup>/L]/[Cu<sup>II</sup>] = 180:1:0.5:0.05. 25% solvent (by volume, anisole) at 80 °C. [I] is based on 100% functionalization of backbone.

<sup>b</sup> Based on linear standards of poly(styrene). <sup>c</sup> First column, CHCl<sub>3</sub> eluent; second column, THF eluent. <sup>d</sup> THF as the eluent. <sup>e</sup> 0.025 equiv of CuBr<sub>2</sub> were placed in flask A and flask B.

**Figure 3.** <sup>1</sup>H NMR spectra: (A) compound **6**; (B) compound **5**, which shows covalent linkage of the pMA to the PT.**Figure 4.** GPC analysis displaying a number distribution of **5**, pMA arms, and **6**, showing a clean shift to higher molecular weights.

could not be analyzed with chloroform as the eluent because of insufficient column length and porosity (see Materials and Characterization; Waters 2690 GPC).

To determine the content of ATRP initiator in **5**, <sup>1</sup>H NMR and GPC analyses were utilized. <sup>1</sup>H NMR spectroscopy was first used on **5** to determine the ratio between the proton integration at 4.0–4.2 ppm and the integration at 7 ppm. Assuming the polymer achieved full functionality, the ratio should be 3:1. The percent functionality could then be found by dividing the experimental ratio by the theoretical ratio (see Table 1). To confirm functionality, further analysis was completed. From the GPC analysis of **5** using CHCl<sub>3</sub> as the eluent and the predicted functionality, one can approximate the degree of polymerization (DP) of the PT chain. Knowing the number of aromatic protons from the DP and completing the <sup>1</sup>H NMR analysis of **6** from 6.8 to 7.2 ppm, one can determine the area per proton,

which can be compared to the region between 3.4 and 3.8 ppm to determine the total number of MA repeat units per PT chain. From the calculated macroinitiator functionality and the total number of MA repeat units per chain, an experimental molecular weight of the grafts can be determined (see Table 1, NMR column).

Table 1 compares the molecular weight data of the sidearms as determined by the GPC and <sup>1</sup>H NMR analyses. The functionality of **5** will determine the initiator concentration and, ultimately, the molecular weight of the sidearms. Therefore, the theoretical molecular weights of the sidearms were determined assuming that the PT attained 100% functionality (Theo{100%}) and using the functionality calculated from the <sup>1</sup>H NMR analysis (Theo{Actual}). Large inconsistencies arise in comparisons of the GPC and NMR molecular weights to the Theo{100%} molecular weight, indicating that the chain is not 100% functionalized. However, there is agreement within experimental error between the GPC and NMR molecular weights and the Theo{Actual} molecular weights, which supports the calculated functionality of **5**. Functionality cannot be determined solely from GPC analysis of the grafts. It should be noted that all GPC analysis was completed against linear poly(styrene) standards using an internal standard. This method does demonstrate controlled growth of the sidearms, i.e., low PDI and uniform Gaussian distribution, but does not report the true molecular weights of the graft copolymers. This analysis will skew the molecular weights of polymers of different topologies. For example, star, branched, and graft copolymers such as **6** will display lower molecular weights than their linear analogues as a result of the grafting density.<sup>36,41</sup> Therefore, it is very likely that the reported molecular weights of the graft copolymers have been dramatically underestimated. Because the molecular weights of the graft copolymers are not accurate, it is not possible to derive the functionality solely from GPC analysis.

By isolating the PT chains within pMA, interesting optical properties could be enhanced. UV/vis analysis was performed on **5** and **6** in solution and in the solid state. From the absorbance spectrum, one can qualitatively determine the conjugation length of the PT, where a red shift indicates a higher conjugation length. From Figure 5, **5** and **6** behave similarly in solution. Both are well solvated in chloroform, which disrupts conjugation and reduces the conjugation length. However, in the solid state, the two behave differently. The dropcast film of **5** behaves as expected, showing a red shift related to an increase in conjugation length from PT–PT  $\pi$ -stacking interactions. A dropcast film of **6** absorbs at the same wavelength as well-solvated PT, corresponding to a disordered array of PT and a lower conjugation length. In the dropcast graft copolymer film, the large polymer



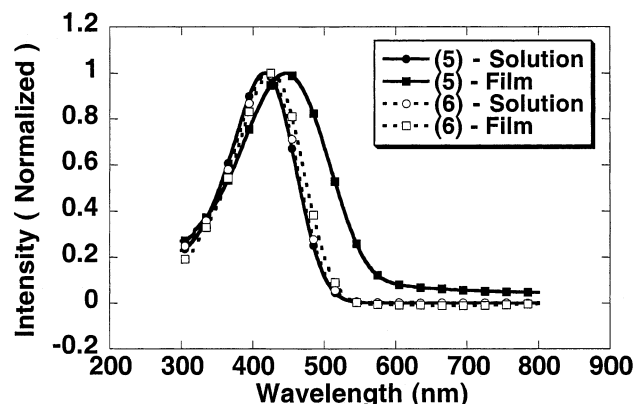


**Figure 5.** UV/vis analysis (300–700 nm) of **5** and **6** in solution and as cast films.

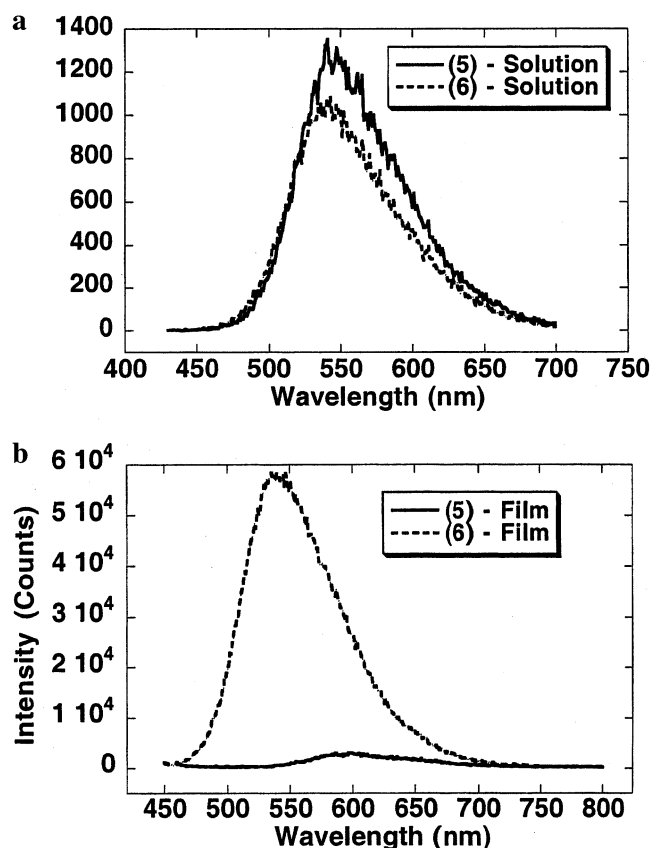


**Figure 6.** Fluorescence of **5** and **6** in solution excited at 420 nm and as cast films excited at 445 and 420 nm, respectively.

side chains twist and separate the PT chains, forming a pMA matrix that effectively traps the PT in a solution conformation.

Fluorescence studies were conducted in solution and in the solid state, and the results are similar to the UV/vis analysis (see Figure 6). In solution, **5** and **6** fluoresced at the same wavelength with the same magnitude. In the solid state, **5** showed minimal fluorescence, whereas **6** demonstrated a blue-shifted fluorescence spectrum of approximately 20 times greater intensity. A possible explanation for the quenching of fluorescence in **5** is the packing of the PT in the solid state. Well-packed PT can allow aggregates to form, which trap excitations of the polymer chain in a nonfluorescent state. This is consistent with the red-shifted absorption spectrum in Figure 5 suggesting a more ordered solid-state system for **5**. Recently published results confirm

this conclusion of fluorescence quenching through  $\pi$ -stacking interactions.<sup>22,42</sup> The pMA sidearms act to separate the PT backbones and inhibit any aggregation, which improves the fluorescent capabilities.

An important characteristic of fluorescent materials is the quantum yield, which can be defined as the number of photons emitted compared to the number of photons absorbed. To determine the quantum yield, a spincoated film of pyrene in a poly(methyl methacrylate) matrix was prepared and analyzed. The quantum yield of pyrene in pMMA is a known quantity ( $\Phi = 0.85$ ),<sup>43</sup> and therefore, it can be used as a reference to determine the quantum yield of unknown films.<sup>44</sup> A spincoated film of **6** was prepared, analyzed, and determined to have photoluminescent (PL) quantum yield boundaries of 25–40%. Typical quantum yields of PT are approximately 2%,<sup>13</sup> although previously published results have shown an increase to 24% through molecular modifications of the PT or the PT backbone.<sup>13,17,45,46</sup>

## Conclusions

Graft copolymers containing a PT backbone and pMA side chains were prepared. Up to 90% of the PT backbone was successfully functionalized with ATRP initiating sites. Growth of the pMA side chains from the PT backbone was controlled, yielding low polydispersities and predictable molecular weights. Addition of the sidearms increased the solubility and processability of the material. The sidearms also acted to trap the PT in a solution conformation, thus separating the PT and preventing  $\pi$ -stacking interactions. This was demonstrated by UV/vis spectroscopy and fluorimetry. By preventing aggregation of the PT, nonradiative decay pathways for excited polymer chains were minimized, thus leading to a greater than 20-fold enhancement of fluorescence relative to that of **5** in the solid state. Measurements and analysis of **6** resulted in a quantum yield of up to 40%.

## Materials and Characterization

Methyl acrylate (MA, Acros, 99%) was dried over  $\text{CaH}_2$  and then distilled at ambient temperature.  $\text{CuBr}$  (Acros, 98%) was washed with glacial acetic acid, followed by absolute ethanol and ethyl ether, and then dried under vacuum.<sup>47</sup> All other materials were used as received. Purging consisted of bubbling  $\text{N}_2$  through the solution for approximately 15 min before introducing the solution into the flask.

Monomer conversion was determined using a Shimadzu GC 14-A gas chromatograph equipped with a Megabore column. Injector and detector were kept at a constant temperature of 250 °C, with the column starting at a temperature of 40 °C for 2 min and being heated to 180 °C at a rate of 40 °C/min.

Polymer molecular weights were estimated using a GPC system equipped with a Waters WISP 712 autosampler, Polymer Standards Service columns (guard,  $10^2$  Å,  $10^3$  Å,  $10^4$  Å, and  $10^5$  Å), and a Waters 410 RI detector against linear poly(styrene) in THF (1 mL/min) at 35 °C using toluene as an internal standard. GPC data were also recorded on a Waters 2690 separation module equipped with a Waters 2487 dual-wavelength absorbance UV detector and Phenogel columns (guard,  $10^2$  Å, and  $10^4$  Å) calibrated against linear poly(styrene) in  $\text{CHCl}_3$  (1 mL/min).

$^1\text{H}$  NMR characterization was performed in  $\text{CDCl}_3$  (using TMS as an internal standard) on a Bruker 300-MHz instrument.

UV/vis analysis was conducted on a Perkin-Elmer Lambda 900 spectrometer. Solutions of **5** and **6** were prepared ( $\sim 0.01$  mg/mL) in  $\text{CHCl}_3$  and analyzed from 300 to 700 nm. Thin films of backbone and brush were dropcast from solution onto glass slides and analyzed from 300 to 700 nm.

Fluorescence studies of solutions **5** and **6** were conducted on a Photon Technology International Fluorimeter PTI Master instrument. Dilute solutions ( $\sim 0.01$  mg/mL) in  $\text{CHCl}_3$  were prepared and analyzed at an excitation wavelength of 420 nm with a spectrum range from 430 to 700 nm using a step of 1 nm and an integration time of 5 ms at a frequency of 100 Hz.

Solid-state fluorescence studies of **5** and **6** were conducted on a Jobin YUON-SPEX FluoroMax-2 fluorimeter. Thin films were prepared by dropcasting dilute solutions onto glass slides. The excitation wavelengths used were 445 and 420 nm for **5** and **6**, respectively. Spectrum ranges were 460–800 and 450–800 nm using a step of 1 nm and an integration time of 0.1 s for **5** and **6**, respectively. Corrections adjusting for different excitation wavelength intensities were made via the fluorimeter acquisition software.

Photoluminescent (PL) quantum yield measurements were performed as follows: A solution of pyrene and poly(methyl methacrylate) (PMMA) in THF was prepared [pyrene ( $\Phi = 0.85$ ),  $\sim 0.01$  mg/mL; PMMA,  $\sim 1$  mg/mL].<sup>43</sup> Solutions of this standard and **6** were spincoated onto glass slides. Absorption spectra were then recorded for each, followed by fluorescence emission spectra. The pyrene standard was excited at 307 nm, and **6** was excited at 420 nm. The quantum yield was then calculated as described by Osaheni et al.<sup>44</sup>

## Experimental Section

**Preparation of Thiophene Monomer.** *2-Bromo-3-(2-hydroxy-1-ethyl)thiophene (2)*. 2-Thienyl-1-ethanol (Aldrich, 99%) (5.00 g, 39.0 mmol) was dissolved in tetrahydrofuran (THF) (50 mL) in a flask and placed in an ice bath. *N*-Bromosuccinimide (Aldrich, 99%) (7.10 g, 39.6 mmol) was added portionwise to the flask, and the suspension was stirred for 2 h. The reaction mixture was washed with water ( $3 \times 100$  mL) and dried over anhydrous  $\text{MgSO}_4$  (Fisher), and then the solvent was removed under vacuum. Compound **2** was isolated as a colorless oil (8.56 g, 95% yield) after vacuum distillation (67 °C, 0.05 Torr).

GC-MS [ $M^+$ ] ( $m/z$ ): 208 (d), 177 (d), 127 (s), 97 (s).

<sup>1</sup>H NMR: 1.47 (s, 1 H, OH), 2.86 (t,  $J = 6$  Hz, 2H,  $\text{TpCH}_2$ ), 3.83 (t,  $J = 7$  Hz, 2H,  $\text{TpCH}_2\text{CH}_2\text{OH}$ ), 6.87 (d,  $J = 5$  Hz, 1H,  $\text{TpH}$ , 4 position), 7.22 (d,  $J = 5$  Hz, 1H,  $\text{TpH}$ , 5 position).

*2-Bromo-3-(2-trimethylsiloxy-1-ethyl)thiophene (3)*. In a flask under nitrogen, **2** (7.00 g, 33.7 mmol) was dissolved in THF (100 mL). Triethylamine ( $\text{NEt}_3$ , Acros, 99%) (6.80 g, 2 equiv) was added via syringe to the solution, and the mixture was stirred for 15 min. Next, trimethylsilyl chloride (Aldrich, 98%) (3.67 g, 1 equiv) was injected into the reaction flask, and the reaction mixture was stirred for 20 h. The reaction mixture was then diluted with ether (200 mL) and washed with water ( $2 \times 75$  mL), aqueous HCl (0.2 M,  $2 \times 100$  mL), and finally water ( $1 \times 100$  mL). The organic layer was dried over anhydrous  $\text{MgSO}_4$  and filtered, and the solvent was removed, giving a colorless liquid (8.71 g, 92% yield). The compound was subsequently used without further isolation.

GC-MS [ $M^+$ ] ( $m/z$ ): 280 (d), 265 (d), 199 (s), 103 (s), 73 (s).

<sup>1</sup>H NMR: 0.08 (s, 9H,  $\text{OSi}(\text{CH}_3)_3$ ), 2.81 (t,  $J = 7$  Hz, 2H,  $\text{TpCH}_2$ ), 3.74 (t,  $J = 7$  Hz, 2H,  $\text{TpCH}_2\text{CH}_2\text{O}-$ ), 6.85 (d,  $J = 5$  Hz, 1H,  $\text{TpH}$ , 4 position), 7.18 (d,  $J = 5$  Hz, 1H,  $\text{TpH}$ , 5 position).

**Preparation of PT.** *2,5-Poly[3-(2-trimethylsiloxy-1-ethyl)thiophene] (4)*. THF (50 mL) and **3** (2.50 g, 9.00 mmol) were added to a flask under nitrogen and cooled to  $-70$  °C. Separately, diisopropylamine (1.25 mL, 1 equiv) was dissolved in THF (10 mL), and *n*-butyllithium (2.5/hexane, 3.6 mL, 1 equiv) was added dropwise. The resulting mixture was then transferred slowly into the first flask via cannula, keeping the reaction temperature below  $-60$  °C. The reaction mixture was stirred for 30 min, and anhydrous zinc chloride (beads, 1.22 g, 1 equiv) was added. After 45 min, the solution was warmed to room temperature, and a catalytic amount of [1,3-bis-(diphenylphosphino)propane]dichloronickel(II) ( $\text{Ni}(\text{dppp})\text{Cl}_2$ ) (20 mg) was added. The reaction mixture was stirred for 16 h, when the reaction was then quenched by precipitation of the resulting polymer in methanol, followed by subsequent Soxhlet

extractions (methanol, hexanes, chloroform) to recover a red powder from the hexanes fraction (153 mg, 8.5% yield). NMR data of the polymer were not recorded because of solubility problems.

**ATRP Functionalization of PT.** *2,5-Poly[3-[1-ethyl-2-(2-bromopropionate)]thiophene] (5)*. To a flask under nitrogen were added polymer **4** (hexane fraction, 153 mg, 0.77 mmol) and THF (100 mL). Then, 2-bromo-propionyl bromide (0.5 mL, 1.1 equiv),  $\text{NEt}_3$  (0.2 mL, 1 equiv), and tetrabutylammonium fluoride (1.0 M/THF, 1 equiv), in that order, were added to the flask via syringe. The reaction mixture was stirred for 16 h and then precipitated in methanol, filtered, and subjected to subsequent Soxhlet extractions (methanol, THF) to recover a purple powder from the THF fraction.

<sup>1</sup>H NMR: 0.08 (s, 1.2 H,  $\text{OSi}(\text{CH}_3)_3$ ), 1.88 (br, 2.6 H,  $\text{CHBrCH}_3$ ), 2.99 (br, 0.26 H,  $\text{CH}_2\text{CH}_2\text{OTMS}$ ), 3.14 (br, 2 H,  $\text{CH}_2\text{CH}_2\text{OTMS}$  and  $\text{CH}_2\text{CH}_2\text{OCO}$ ), 4.14 (br, 0.87 H,  $\text{CHBr}$ ), 4.18 (br, 1.74 H,  $\text{CH}_2\text{CH}_2\text{OC}$ ), 7.06 (br, 1 H,  $\text{CH}$ , 4 position).

**ATRP of pMA Grafts.** *2,5-Poly[3-[1-ethyl-2-(2-[poly(methyl acrylate)] propionate)] thiophene] (6)*. Polymer **5** (0.20 g, 0.77 mmol Br),  $\text{CuBr}_2$  (4.5 mg, 0.019 mmol) and a stir bar were placed into a 25-mL round-bottom flask (A), and then vacuum/backfilled with  $\text{N}_2$  ( $5 \times$ ). Purged anisole (4 mL) was then added to flask A via a purged syringe. Into a second 25-mL round-bottom flask (B) were placed  $\text{CuBr}$  (54.7 mg, 0.38 mmol),  $\text{CuBr}_2$  (4.5 mg, 0.019 mmol) and a stir bar. Flask B was then vacuum/backfilled with  $\text{N}_2$  ( $5 \times$ ). Next, purged methyl acrylate (12.5 mL, 138 mmol) and purged *N,N,N',N',N'*-pentamethyldiethyltri-amine (PMDETA) (65.4 mg, 0.38 mmol) were added via purged syringe. For the addition of PMDETA, the empty syringe was first weighed, filled with PMDETA, weighed again, tared, and then weighed after the PMDETA had been added to the flask. The contents of flask B were stirred until homogeneous. The mixture in flask B was then transferred to flask A via a purged syringe. Flask A was then placed into an oil bath at 80 °C for 145 min. Samples were taken for analysis by GC (19%), GPC ( $M_n = 44\,000$  g/mol, PDI = 1.22), and NMR spectroscopy. The remaining reaction mixture was dissolved in acetone and passed through a column of alumina. Excess solvent was removed, and then the polymer was precipitated in a 50:50 MeOH/ $\text{H}_2\text{O}$  mixture.

<sup>1</sup>H NMR: 0.08 (s, 1 H,  $\text{OSi}(\text{CH}_3)_3$ ), 0.89–2.41 (br, 164.3 H,  $\text{CH}_2\text{CH}$ ), 3.63 (br, 117.2 H,  $\text{OCH}_3$ ), 4.08 (br, 0.8 H,  $\text{CHBr}$ ), 4.11 (br, 1.6 H,  $\text{CH}_2\text{OC}$ ), 6.92–7.26 (br, 1 H,  $\text{CH}$ , 4 position).

**Cleavage of pMA Grafts from PT.** Polymer **6** (0.180) and a stir bar were placed into a 25-mL round bottom flask. THF (5 mL) was then added. MeOH (11.5 mL) was then added to the flask, which caused precipitation of the graft copolymer. THF (1 mL) was then added to redissolve the polymer.  $\text{H}_2\text{SO}_4$  (10 drops) was added to the flask. The solution was then placed into an oil bath at 75 °C for 5 days. The mixture was then dissolved in acetone, filtered to remove insoluble PT, and precipitated in 50:50 MeOH/ $\text{H}_2\text{O}$ . An analytical sample was isolated and analyzed by GPC ( $M_n = 5300$  g/mol, PDI = 1.07).

**Acknowledgment.** The authors acknowledge and thank Prof. McCullough and Prof. Matyjaszewski for their support and guidance and for the opportunity to work in their labs. We also thank Prof. Armitage and Prof. Kowalewski for their helpful comments and criticism. We thank Prof. Peteanu and Pushon Chowdrowy for help with quantum yield measurements and calculations, as well as Prof. Patten, Dr. Kelly Davis, Dr. Jeff Pyun, Dr. Jinsong Liu, and Dr. Dan Savin for helpful discussions. We acknowledge the Howard Hughes Medical Institute, CRP Consortium, and NSF [Grants CHE-9807707 (R.D.M.) and DMR-0090409 (K.M.)] for funding.

## References and Notes

- Shirikawa, H.; Louis, E. J.; MacDiarmid, A. G.; Chiang, C. K.; Heeger, A. J. *J. Chem. Soc., Chem. Commun.* **1977**, 579.
- Garnier, F.; Hajlaoui, R.; Yassar, A.; Srivastava, P. *Science* **1994**, *265*, 1864.

- (3) Novak, P.; Muller, K.; Santhanam, K. S. V.; Haas, O. *Chem. Rev.* **1997**, *97*, 207.
- (4) Burroughes, J. H.; Bradley, D. D. C.; Brown, A. R.; Marks, R. N.; Mackay, K.; Friend, R. H.; Burns, P. L.; Holmes, A. B. *Nature* **1990**, *347*, 539.
- (5) Crone, B.; Dobalapur, A.; Lin, Y.-Y.; Filas, R. W.; Bao, Z.; LaDuca, A.; Sarpeshkar, R.; Katz, H. *Nature* **2000**, *403*, 521.
- (6) McQuade, D. T.; Pullen, A. E.; Swager, T. M. *Chem. Rev.* **2000**, *100*, 2537.
- (7) Olinga, T.; Francois, B. *Makromol. Chem., Rapid Commun.* **1991**, *12*, 575.
- (8) Francois, B.; Olinga, T. *Synth. Met.* **1993**, *57*, 3489.
- (9) Hallensleben, M.; Hollwedel, F.; Stanke, D. *Macromol. Chem. Phys.* **1995**, *196*, 3535.
- (10) Alkan, S.; Toppare, L.; Hepuzer, Y.; Yagci, Y. *J. Polym. Sci. A: Polym. Chem.* **1999**, *37*, 4218.
- (11) Ranieri, N.; Ruggeri, G.; Ciardelli, F. *Polym. Int.* **1999**, *48*, 1091.
- (12) Waugaman, M.; Pratt, L.; Khan, I. *Polym. Prepr.* **1997**, *38*, 257.
- (13) Pei, J.; Yu, W.-L.; Huang, W.; Heeger, A. J. *Macromolecules* **2000**, *33*, 2462.
- (14) Bao, Z.; Amundson, K. R.; Lovinger, A. J. *Macromolecules* **1998**, *31*, 8647.
- (15) Yang, J.; Swager, T. M. *J. Am. Chem. Soc.* **1998**, *120*, 5321.
- (16) Son, S.; Dodabalapur, A.; Lovinger, A. J.; Galvin, M. E. *Science* **1995**, *269*, 376.
- (17) Ingnas, O.; Granlund, T.; Theander, M.; Berggren, M.; Anderson, M. R.; Ruseckas, A.; Sundstrom, V. *Opt. Mater.* **1998**, *9*, 104.
- (18) Berggren, M.; Gustafsson, G.; Inganaes, O.; Andersson, M. R.; Wennerstrom, O.; Hjertberg, T. *Adv. Mater.* **1994**, *6*, 488.
- (19) Gettinger, C. L.; Heeger, A. J.; Drake, J. M.; Pine, D. J. *J. Chem. Phys.* **1994**, *101*, 1673.
- (20) Hsieh, B. R.; Yu, Y.; Forsythe, E. W.; Schaaf, G. M.; Feld, W. A. *J. Am. Chem. Soc.* **1998**, *120*, 231.
- (21) Rothberg, L. J.; Yan, M.; Son, S.; Galvin, M. E.; Kwock, E. W.; Miller, T. M.; Katz, H. E.; Haddon, R. C.; Papadimitrakopoulos, F. *Synth. Met.* **1996**, *78*, 231.
- (22) Kim, J.; Swager, T. M. *Nature* **2001**, *411*, 1030.
- (23) Chen, X. L.; Jenekhe, S. A. *Macromolecules* **1996**, *29*, 6189.
- (24) Yan, M.; Rothberg, L. J.; Kwock, E. W.; Miller, T. M. *Phys. Rev. Lett.* **1995**, *75*, 1992.
- (25) Sun, B. J.; Miao, Y.-J.; Bazan, G. C.; Conwell, E. M. *Chem. Phys. Lett.* **1996**, *260*, 186.
- (26) Hu, B.; Karasz, F. E. *Synth. Met.* **1998**, *92*, 157.
- (27) Smilowitz, L.; Hays, A.; Heeger, A. J.; Wang, G.; Bowers, J. E. *J. Chem. Phys.* **1993**, *98*, 6504.
- (28) Malenfant, P.; Frechet, J. *Macromolecules* **2000**, *33*, 3634.
- (29) Chen, F.; Mehta, P. G.; Takiff, L.; McCullough, R. D. *J. Mater. Chem.* **1996**, *6*, 1763.
- (30) McCullough, R. D.; Lowe, R. D. *J. Chem. Soc., Chem Commun.* **1992**, 70.
- (31) McCullough, R. D.; Tristram-Nagle, S.; Williams, S. P.; Lowe, R. D.; Jayaraman, M. *J. Am. Chem. Soc.* **1993**, *115*, 4910.
- (32) McCullough, R. D.; Williams, S. P.; Tristram-Nagle, S.; Jayaraman, M.; Ewbank, P. C.; Miller, L. *Synth. Met.* **1995**, *69*, 279.
- (33) Wang, J. S.; Matyjaszewski, K. *Macromolecules* **1995**, *28*, 7901.
- (34) Wang, J. S.; Matyjaszewski, K. *J. Am. Chem. Soc.* **1995**, *117*, 5614.
- (35) Patten, T.; Xia, J.; Abernathy, T.; Matyjaszewski, K. *Science* **1996**, *272*, 866.
- (36) Beers, K.; Gaynor, S.; Matyjaszewski, K.; Sheiko, S.; Moller, M. *Macromolecules* **1998**, *31*, 9413.
- (37) Boerner, H.; Beers, K.; Matyjaszewski, K.; Sheiko, S.; Moller, M. *Macromolecules* **2001**, *34*, 4375.
- (38) Yu, J.; Orfino, F. P.; Holdcroft, S. *Chem. Mater.* **2001**, *13*, 526.
- (39) Yu, J.; Holdcroft, S. *Macromolecules* **2000**, *33*, 5073.
- (40) Fischer, H. *Macromolecules* **1997**, *30*, 5666.
- (41) Tsitsilianis, C.; Ktoridis, A. *Macromol. Rapid Commun.* **1994**, *15*, 845.
- (42) Gaylord, B. S.; Wang, S.; Heeger, A. J.; Bazan, G. C. *J. Am. Chem. Soc.* **2001**, *123*, 6417.
- (43) Guibault, G. ., Ed. *Practical Fluorescence*, 2nd ed.; Marcel Dekker: New York, 1990.
- (44) Osaheni, J. A.; Jenekhe, S. A. *J. Am. Chem. Soc.* **1995**, *117*, 7389.
- (45) Granlund, T.; Theander, M.; Berggren, M.; Andersson, M.; Ruseckas, A.; Sundstrom, V.; Bjork, G.; Granstrom, M.; Inganas, O. *Chem. Phys. Lett.* **1998**, *288*, 879.
- (46) Gigli, G.; Barbarella, G.; Favaretto, L.; Cacialli, F.; Cingolani, R. *Appl. Phys. Lett.* **1999**, *75*, 439.
- (47) Keller, R. N.; Wycoff, H. D. *Inorg. Synth.* **1946**, *2*, 1.

MA011638D